*Journal of Pharmaceutical & Biomedical Analysis*
Vol. 8, No. 6, pp. 477–491, 1990
Printed in Great Britain

0731–7085/90 $3.00 + 0.00


# Chemiluminescence: a sensitive and versatile method for analyte detection*

RICHARD S. GIVENS,† DAVID A. JENCEN,‡ CHRISTOPHER M. RILEY, JOHN F. STOBAUGH, HITESH CHOKSHI§ and NOBUAKI HANAOKA‖

*The Center for Bioanalytical Research, The University of Kansas, Lawrence, KS 66045, USA*

**Abstract**: The generation of light from the oxidation of oxalic esters with hydrogen peroxide has been applied to the detection of luminescent materials. In order to improve the efficiency of this method, which is <0.1%, and to enhance the selectivity for target analytes, an in-depth investigation of the oxalate ester–hydrogen peroxide reaction has been conducted. A kinetic model has been developed based on the effects of catalysts, reagents and reaction conditions for maximum light production. Application of the model to liquid chromatography through the "time-dependent emission window" concept affords a predictable maximum sensitivity for selected analytes.

Application to the detection and quantitation of met- and leu-enkephalins which have been labelled with naphthalene-2,3-dicarboxyaldehyde/cyanide provides support for this methodology. Other bioanalytical applications are presented.

**Keywords**: *Chemiluminescence; liquid chromatography; peroxyoxalate; naphthalene-2,3-dialdehyde/cyanide; dioxetanedione; imidazole catalysis, mechanisms, activation energies; enkephalins; neurotensins.*

## Introduction

Chemical activation of emission from fluorescent analytes appears to have great promise for increasing the sensitivity of detection for liquid chromatography (LC), flow injection analysis (FIA), and a variety of other assay methods. In principle, chemiluminescence, generated by addition of certain oxidants to solutions containing fluorescent materials, should be applicable to any fluorescence-based detection method. The fact is, however, that this exaggerates the potential of the chemiluminescence method. A number of important limitations, both practical and theoretical, preclude the generality of chemical activation of fluorescence. Nevertheless, the lure of enhanced sensitivity reported in certain instances has encouraged several research groups to enter the chemiluminescence arena [1–5].

In 1980, Kobayashi and Imai [1] began the quest for a general chemiluminescence method for LC detection with the oxalate ester–hydrogen peroxide reaction in order to produce fluorescence from several well-known analyte labels. In those early studies, low limits of detection of 2 to 5 fmol could be achieved. Subsequent studies in his and the laboratories of Melbin [2], Sigvardson and Birks [3] and others [4, 5] quickly established the sensitivity and potential versatility of the oxalate ester–hydrogen peroxide reaction for luminescence activation. Imai's achievement was seminal, for it introduced chemiluminescence methodology to applications in a wide variety of fluorescence-based assays.

Researchers at the Center for Bioanalytical Research entered the arena in 1985 for precisely the reasons outlined above and because a new fluorogenic derivatizing reagent that reacted with primary amines to form highly fluorescent labelled analytes had been developed [6, 7]. These labelled analytes were subjected to conventional reversed-phase chromatography (RP–LC) for separation and fluorescence detection [8–12].

A pleasant surprise was the achievement of over 70- to 100-fold enhancement in sensitivity in the first experiments with the oxalate–hydrogen peroxide chemiluminescence method [13]. However, it was also abundantly clear that the method had serious limitations and

*Presented at the Analysis of Pharmaceutical Quality (APQ) Section's Symposium of the Fourth Annual Meeting of the American Association of Pharmaceutical Scientists (AAPS), Atlanta, Georgia, October 1989.

† Author to whom correspondence should be addressed.
‡ Present address: Norwich Eaton Pharmaceuticals, Inc., Norwich, NY, USA.
§ Present address: Roche Pharmaceuticals, Inc., Nutley, NJ, USA.
‖ Present address: Shimadzu Corp., Kyoto, Japan.

certain drawbacks. In this presentation, current progress is reported along with results on the oxalate ester–hydrogen peroxide-activated chemiluminescence methodology.

### Fluorogenic Naphthalene-2,3-dialdehyde Reagent

The new reagent [6, 7] developed by the Center involves the reaction of naphthalene-2,3-dialdehyde and cyanide (NDA/CN) with a primary amine to form the highly fluorescent 1-cyano-2-substituted-benz[f]isoindole (CBI-derivative) [7, 8] (in equation 1). The CBI-derivative is relatively stable and usually isolable as a crystalline product which can then be fully characterized. The fluorescence efficiencies of several such derivatives are excellent, varying from 0.3 to 1.0, and are relatively insensitive to a range of prototypical LC solvents [8, 9]. Furthermore, the reagent system has been successfully applied to the derivatization of catecholamines [10], larger peptides [11] and a few small proteins [12]. The absorption and emission characteristics (Fig. 1) are ideal for fluorescence-based detectors. Thus, in several critical ways, the NDA/CN derivatizing system is superior to its well-established predecessor, *ortho*-phthaldehyde (OPA)/thiol methodology [14–16].

In one test of the applicability of the NDA/CN methodology, the derivatization of the opioid peptides, leu- and met-enkephalin, has been examined using this reagent [17, 18]. Derivatization at the N-terminus of these peptides with NDA/CN is shown in Scheme 1. The complex reaction mixture obtained was

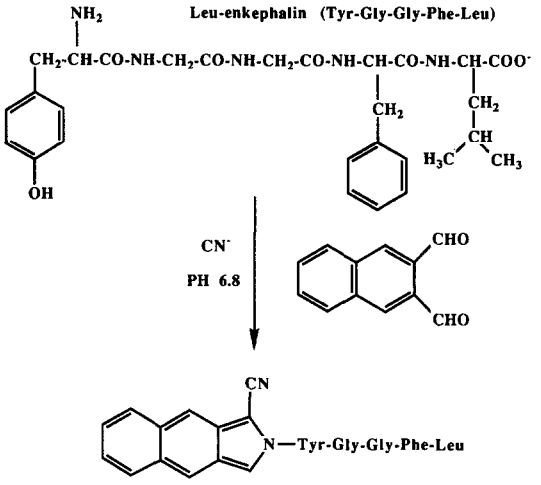


**Scheme 1**
Derivatization reaction for leu-enkephalin.

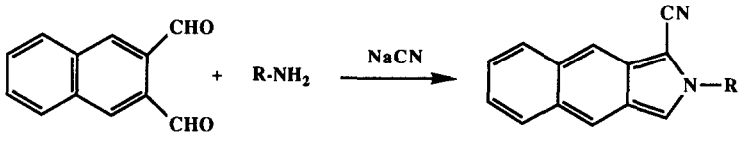


(1)

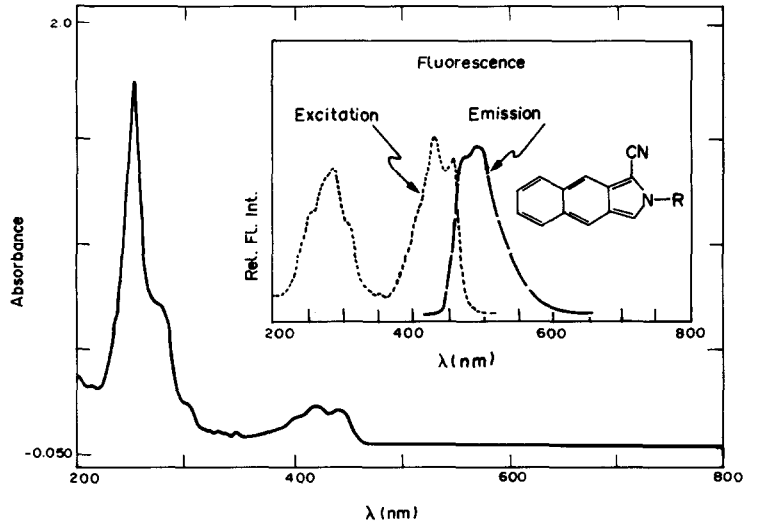


**Figure 1**
Absorption and fluorescence spectra of the cyanobenz[f] isoindole chromophore: CBI-Ala. (Reprinted from ACS Symposium ref. 13 with permission of the American Chemical Society.)

resolved over a two-column tandem arrangement in which column-switching was employed to isolate the two enkephalin derivatives and the internal standard, D-$^2$ala-5-met-enkephalin, from the reaction mixture (Fig. 2) [18]. Even with the improved resolution gained by column-switching, the lowest limits of detection attainable were no better than 1–2 pmol, not low enough to directly detect these opioid peptides at normal plasma levels.

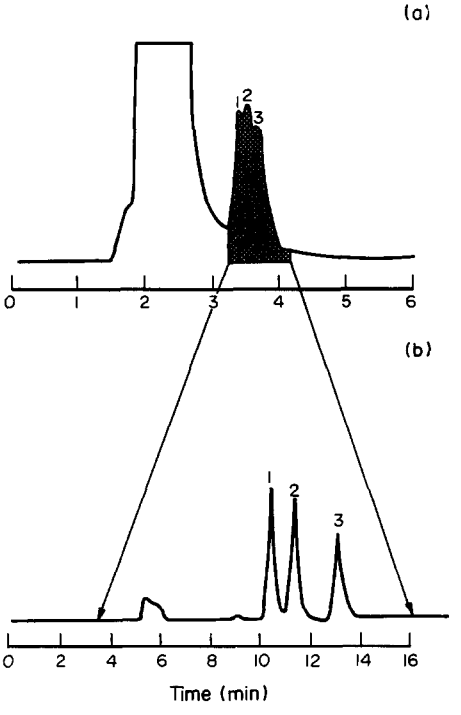


**Figure 2**
LC of met- (**1**), D-$^2$alamet- (**2**) and leu-enkephalin (**3**) on Spherisorb Phenyl (a) and ODS Hypersil (b) by column-switching.

In order to achieve the lower detection limits of 100 fmol injected as required for bioanalysis, chemiluminescence was explored for improved sensitivity. The advantages in increased sensitivity for chemiluminescence over fluorescence derive from the absence of background noise, stray light, instability and Raman emission resulting from the source, as well as background emission from the solvent impurities, all of which contribute to lowering the signal-to-noise ratio at the detector. Chemiluminescence offers an excitation process which is free of the source-related problems. Background emission from impurities does occur, although it can often be reduced by use of filters.

## The Oxalate Ester–Hydrogen Peroxide Chemiluminescence Reaction

### *The Rauhut "dioxetanedione" mechanism*

The reaction of bis-trichlorophenyl oxalate (TCPO) and hydrogen peroxide shown in Fig. 3 typifies known chemiluminescence reactions. Developed at Cyanamid by Rauhut *et al.* [19], this reaction system has become the most frequently employed chemical source for chemiluminescence in LC studies. The general reaction mechanism that evolved from work done by the Cyanamid group and studies by McCapra *et al.* [20] is shown in Scheme 2. Hydrogen peroxide is depicted as reacting with the oxalate to form a "peroxyoxalate" intermediate which then undergoes an intramolecular cyclization and displacement of the second phenolic leaving group. The four-membered ring "dioxetanedione" (**2**), a dimer

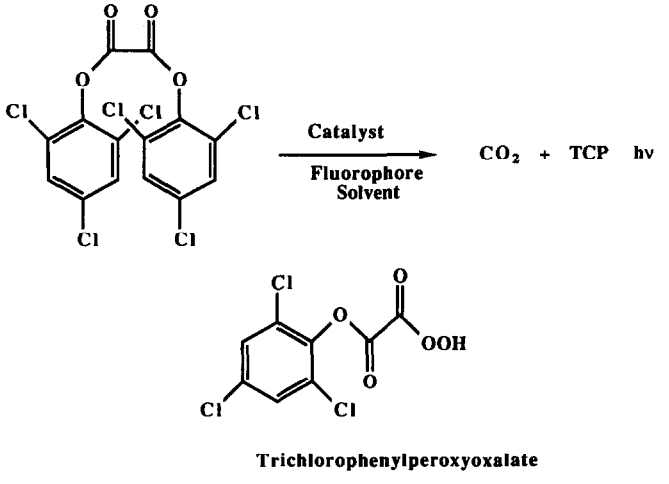


**Figure 3**
The peroxyoxalate chemiluminescence reaction.

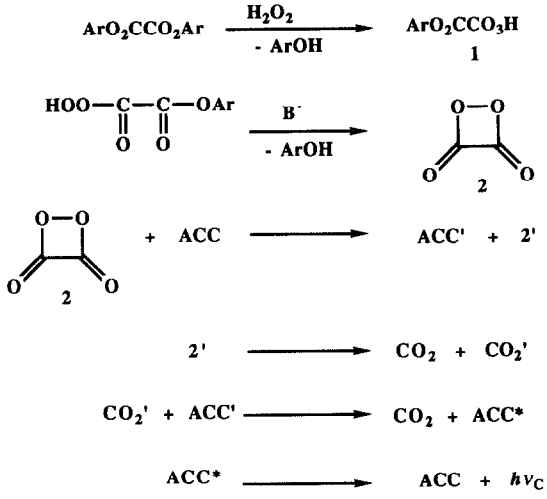


**Scheme 2**
The McCapra–Rauhut Mechanism [20]. ACC is the fluorescent acceptor and $B^-$ is the base catalyst.

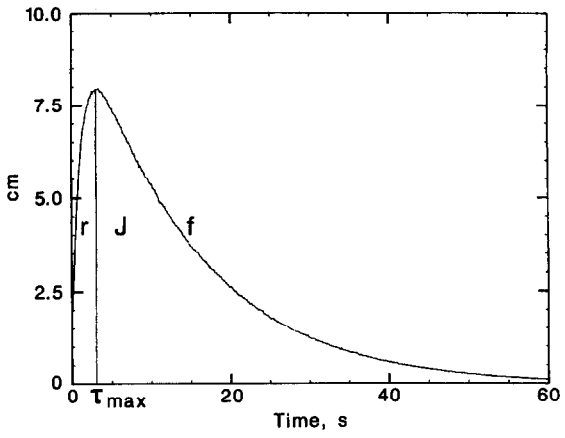


**Figure 4**
A time–intensity profile for the peroxyoxalate chemiluminescence reaction. (Reprinted from ref. 21 with permission of VCH Publishing Co.)

of carbon dioxide, formed in this process has been widely cited as the *key* intermediate in the chemiluminescence mechanism and thus has been the object of much attention by researchers interested in detecting and characterizing this hypothetical reactive intermediate. To date, there is no direct evidence establishing the existence of dioxetanedione [21]. Nevertheless, the folklore concerning its intermediacy persists.

McCapra's contribution [20] to the mechanistic detail was his incorporation of Schuster's chemically induced electron exchange luminescence process (CIEEL) [22] as the pathway for the chemical excitation of the fluorophore. An essential feature of the mechanism is electron transfer from the fluorophore to the dioxetanedione, producing a radical cation–radical anion pair. The dioxetanedionyl radical anion fragments to carbon dioxide and the carbon dioxide radical anion, a much better reducing agent than the dioxetanedionyl radical anion. Back electron transfer to the fluorophore radical cation from the carbon dioxide anion produces the singlet excited state of the fluorophore which subsequently yields the observed fluorescence emission.

*Kinetics of light production*

Chemiluminescence generated in this manner is generally very short-lived. A profile of the fluorescence emission versus time for the TCPO–hydrogen peroxide reaction using 9,10-diphenylanthracene as the fluorophore is given in Fig. 4. Characteristic features of this biexponential curve are the rise ($k_r$) and fall ($k_f$) functions, the time required to reach maximum intensity ($\tau_{max}$), the maximum intensity ($J$) and the luminescence efficiency or area under the curve ($\phi_{CL}$) [20–23]. In aqueous solvents, such as those employed for LC, the lifetime of the chemiluminescence reaction usually persists from a few seconds to 3 min. This short-lived process has important ramifications with respect to applications in a flow system such as encountered with LC. Overlay of the time–intensity profile from stopped-flow experiments with an LC flow profile (Fig. 5) illustrates the importance of both maximizing the chemiluminescence emission and optimizing the light capture by the detector.

Application of the peroxyoxalate technology to the enkephalin problem gained greater assay sensitivity, now affording detection levels as low as 100 fmol for leu-enkephalin as shown in Fig. 6. Direct comparison of the fluorescence and chemiluminescence detection methodologies was impressive. Thus, additional studies on the chemiluminescence reaction appeared warranted because further improvement in the sensitivity was clearly possible.

Recent studies on the mechanism of oxalate–hydrogen peroxide reactions by Palmer, Catherall and Cundall [24], however, have shown that the mechanism proposed by McCapra was incomplete. Palmer *et al.* conclusively demonstrated that the reactive intermediate retained one of the phenolic units by establishing that the rate of generation of the second phenol was directly proportional to the

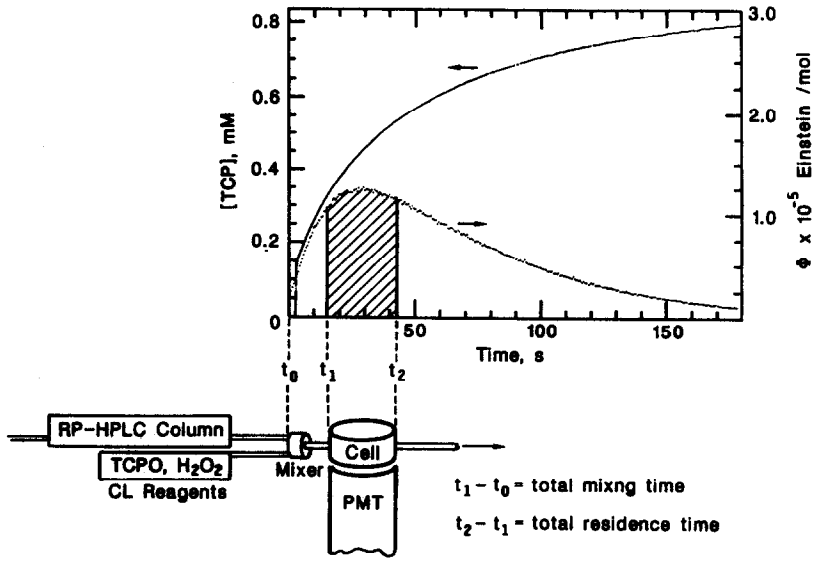


**Figure 5**
Overlay plots of the time–intensity profile and the LC profile. (Reprinted from ref. 21 with permission of VCH Publishing Co.)

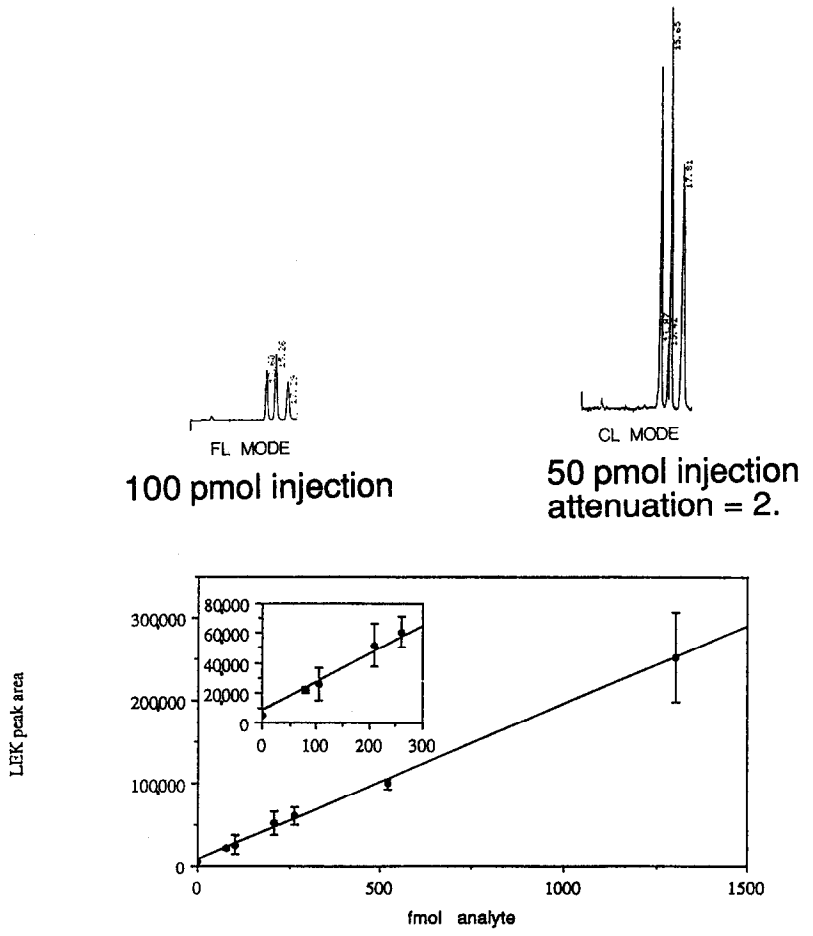


**Figure 6**
Comparison of fluorescence detection for leu- and met-enkephalin. FL = fluorescence and CL = chemiluminescence detector. Inset illustrates the dynamic range of the chemiluminescence response for leu-enkephalin.

rate of chemiluminescence decay [24]. Recent studies at the Center further showed that the notion of a single intermediate responsible for activating the fluorophore by the CIEEL mechanism was inconsistent with complex time–emission profiles found with the TCPO reaction when carried out in organic solvents [25]. Moreover, these recent findings suggested that further mechanistic work is necessary if substantial improvement in the efficacy of the peroxylate reaction is to be attained.

The simplicity of the time–intensity profile in aqueous-based solvents (Fig. 4) invited further study. It was evident that the profile could be accurately modelled by a kinetic treatment for a simple biexponential rise and fall function for the intensity, a model consistent with a two irreversible consecutive step reaction pathway:

$$A \xrightarrow{k_r} [B] \xrightarrow{k_f} C. \qquad (2)$$

Here [B] represents a number of reactive intermediates, or "pooled intermediates" capable of chemical activation of the fluorophore. The aggregate pool is "monitored" by the fluorophore which acts as a probe and reports the aggregate pool as a chemiluminescent signal. Since the time–intensity profile can be very closely modelled by the kinetic sequence for formation and decay of a single intermediate [B], the kinetic behaviour of the mixture of intermediate hydroperoxy oxalates in aqueous-based solvents is adequately represented by the "pooled intermediate" model [21]. The rate constants $k_r$ and $k_f$ are the rise and fall portions of the profile. Such a kinetic treatment provides a time-dependent concentration of the intermediate (or pool of intermediates) to which we have assigned the term M, the structure(s) of which is unknown. The kinetic expression for the time-dependent chemiluminescence intensity $I_{CL}$ is given in equation (3).

$$I_{CL} = \frac{k_r[M]}{k_f - k_r}\left(e^{-k_r t} - e^{-k_f t}\right) \qquad (3)$$

Other physical descriptions of the reaction can be derived from the model expression and the values of the constants derived for $k_r$, $k_f$ and M. For example, the reaction efficiency $\phi_{CL}$ is obtained from the integrated form of equation (3) which is: $\Phi_{CL} = M/k_f$. Likewise, the intensity at the maximum ($J$) of the chemiluminescence profile and the time required to reach the maximum ($\tau_{max}$) are obtained from these constants according to the following expressions:

$$J = M(k_f/k_r)^{(k_f/[k_r - k_f])}, \qquad (4)$$

$$\tau_{max} = \{\ln (k_f/k_r)\}/(k_f - k_r). \qquad (5)$$

With the potential for quantitative assessment of the effect of varying reaction conditions, substrates and catalysts, the five variables considered most important were (1) the nature and concentration of the oxalate, (2) the concentration of hydrogen peroxide (3) the nature and concentration of catalysts, (4) the pH, and (5) the nature and concentrations of mixed aqueous–organic solvents. For each variable, a study of the effect on the time–intensity profile from stopped-flow analyses was modelled by the consecutive reaction kinetic scheme outlined above. Values for $k_r$, $k_f$ and M were obtained and subsequently employed in determining $J$, $\tau_{max}$ and $\phi_{CL}$.

*Studies on the variables for oxalate ester chemiluminescence*

Several new oxalates have been synthesized (K. Nakashima, to be published) in an effort to improve the efficiency for the chemical reaction and to increase the solubility of the esters in mixed aqueous solvents. Among the esters synthesized, the 2,6-difluorophenyl derivative has the best solubility characteristics [26] while retaining the other kinetic features of TCPO. Other oxalates which have been studied include the 2,4-dinitro- and 2,4-difluorophenyl oxalates as well as the more popular 2,4,6-trichloro ester.

In a direct test of the application of model to experiment [27], the effect of concentration of the ester on the rate of the chemiluminescence reaction was determined. As shown in Fig. 7, the maximum $J$ increased with increasing oxalate concentration, whereas the $\tau_{max}$ remained essentially constant, in accord with a first-order dependence on oxalate ester. A similar analysis showed that the effect of hydrogen peroxide on the time–intensity profiles, illustrated in Fig. 8, was complex. For concentrations below 15 mM, the $J$ value increased with $H_2O_2$ concentration in accord with a linear first-order dependence. However,

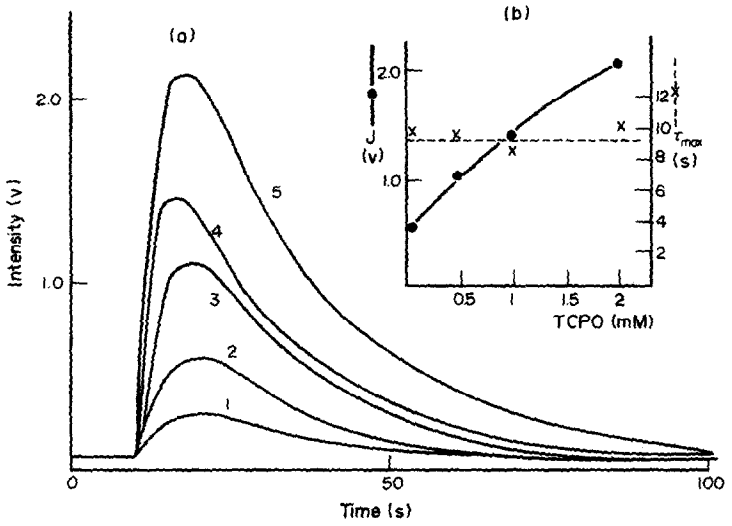


**Figure 7**
(a) The effect of TCPO concentration on the time–intensity profile. Concentration of TCPO: (1) 0.01, (2) 0.02, (3) 0.5, (4) 1.0, (5) 2.0 mM in 40% aqueous $CH_3CN$. Inset (b): The concentration effects on $J$ and $\tau_{max}$.

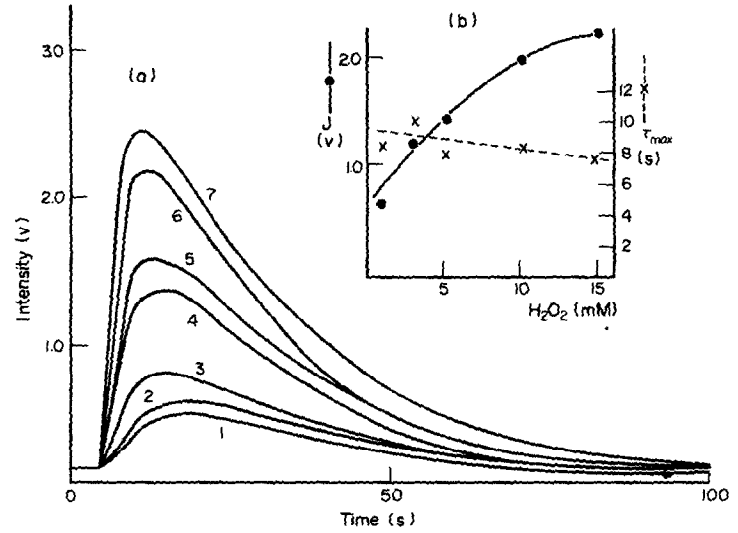


**Figure 8**
(a) The effect of hydrogen peroxide concentration on the time–intensity profile. Concentration of hydrogen peroxide (1) 0.1, (2) 0.5, (3) 1.0, (4) 3.0, (5) 5.0, (6) 10.0, (7) 15.0 mM in 40% aqueous $CH_3CN$. Inset (b): The effect of hydrogen peroxide concentration on $J$ and $\tau_{max}$.

above 30 mM, the $J$ value approached a constant.

The effect of solvents and of pH on the rates and maxima were also complex. The analyses of $H_2O$ concentration (Fig. 9) and pH (Fig. 10) indicated that optimum reaction conditions were 40% aqueous acetonitrile at pH 7.1 for the TCPO–$H_2O_2$ chemiluminescence reaction. These studies and investigations of other oxalates indicated that the optimum pH is approximately equal to the $pK_a$ of the phenol leaving group as anticipated in a normal ester hydrolysis reaction. Thus, the mechanism leading to the hydroperoxy half-ester or peroxyoxalate would appear to be straightforward.

Examinations of a variety of amines as catalysts for the reaction revealed widely different responses (Fig. 11). Simple amines, pyridine and aniline produced a very weak chemiluminescence reaction. However, imidazole gave a much more intense signal which showed an unusual concentration dependence (Fig. 12). Using the "pooled intermediate" model equation, rate constants were deter-

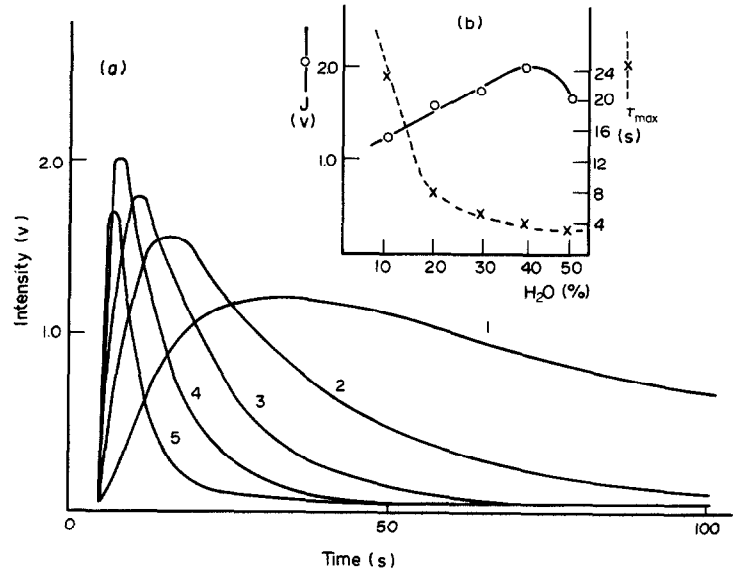


**Figure 9**
(a) The effect of $H_2O$ concentration on the time–intensity profile: (1) 10, (2) 20, (3) 30, (4) 40, (5) 50% (v/v) $H_2O$ in the final solution. Inset (b): The effect of $H_2O$ concentration on $J$ and $\tau_{max}$.

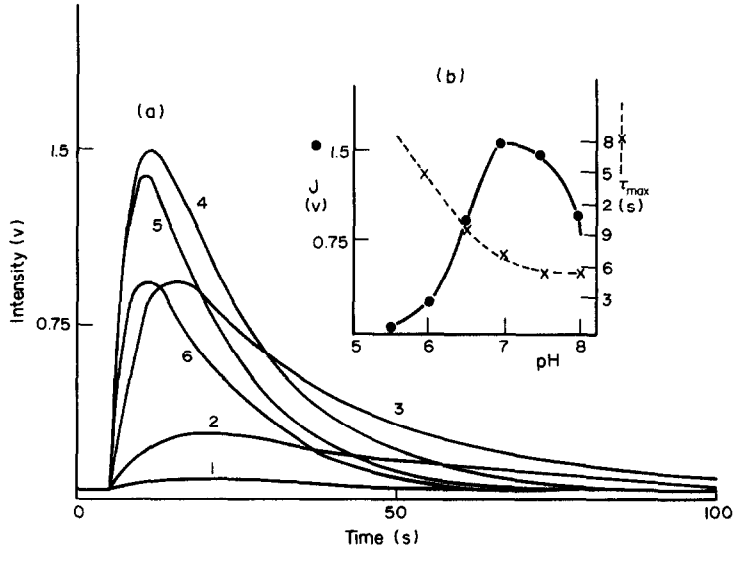


**Figure 10**
(a) pH dependence of the time–intensity profile (1) 5.3, (2) 5.8, (3) 6.3, (4) 6.7, (5) 7.3, (6) 7.7. Inset (b): The effect of pH on $J$ and $\tau_{max}$.

mined as a function of imidazole concentration. As shown in Fig. 13, the rate constant for the rise portion of the curve increased with an increase in imidazole concentration. Interestingly, when the hydrogen peroxide concentration was increased six-fold, a much smaller increase in the catalytic effect was observed. The linear response shown in Fig. 13 gives helpful information about this reaction: (1) The rise rate constant is a combination of a nucleophilic attack by imidazole followed by a rapid reaction with hydrogen peroxide and a general base-catalysed reaction of the oxalate with hydrogen peroxide, i.e.

$$k_r = k_r''[\mathrm{ImH}] + k_r'[\mathrm{ImH}][H_2O_2]. \quad (6)$$

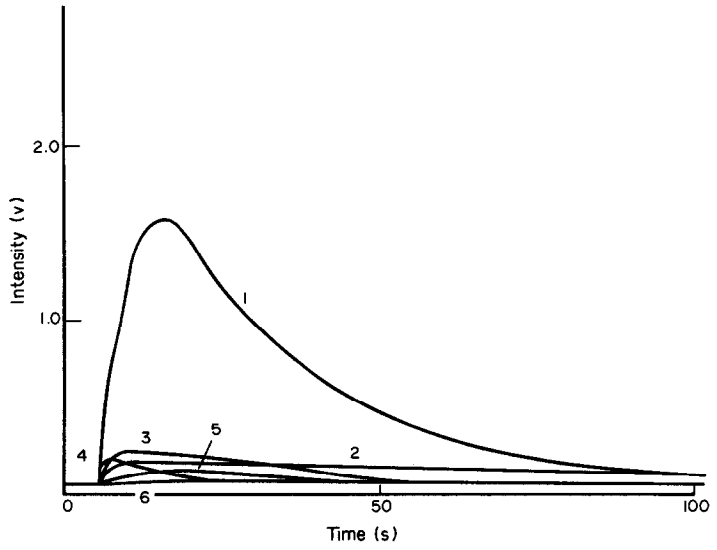


**Figure 11**
The effect of a variety of catalysts on the TCPO–hydrogen peroxide chemiluminescence reaction profile. (1) Imidazole, (2) Tris, (3) triethylamine, (4) pyridine, (5) diethylamine, (6) aniline and all other amines tested (see ref. 27).

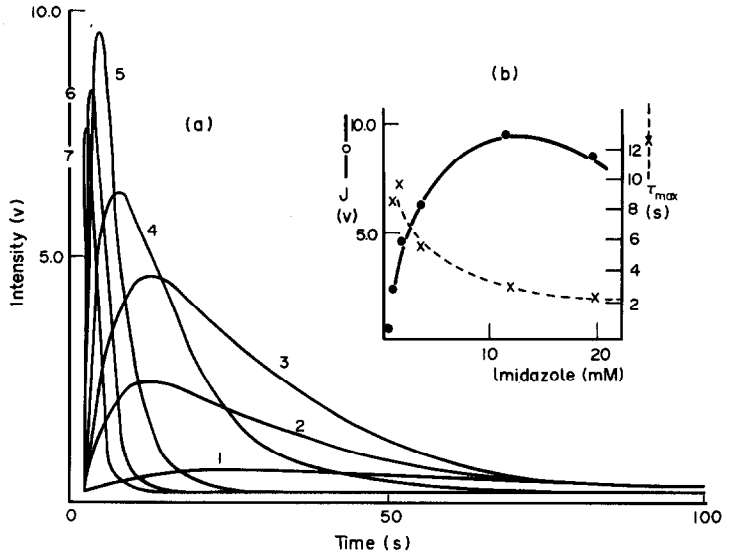


**Figure 12**
(a) The effect of imidazole concentration on the time–intensity profile. (1) 0.4, (2) 1.2, (3) 2.0, (4) 4.0, (5) 12.0, (6) 20.0, (7) 40.0 mM imidazole. Inset (b): The effect of imidazole concentration on $J$ and $\tau_{max}$.

(2) Likewise, there are two processes competing in the decay of the intermediate — a non-imidazole-dependent process and a second-order imidazole-catalysed process, i.e.

$$k_f = k_r' + k_f''[\mathrm{ImH}]^2. \quad (7)$$

*Proposed mechanism for oxalate ester–hydrogen peroxide chemiluminescence*

A new mechanistic scheme [23] which incorporates all of these findings is given in Scheme 3. The mechanism depicts two parallel routes to the peroxyoxalate intermediate in com-

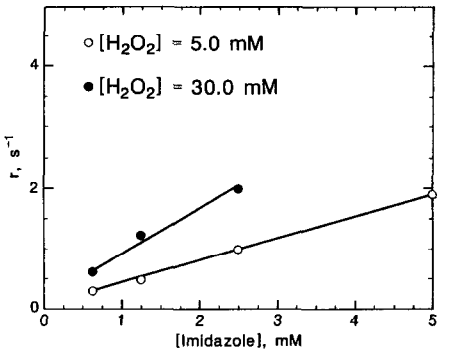


**Figure 13**
The effect of imidazole concentration on $k_r$ ($r$) at two different concentrations of hydrogen peroxide. (Reprinted from ref. 23 with permission of the American Chemical Society.)

petition with hydrolytic reactions of the oxalate. Likewise, reactions of the peroxyoxalate divide into productive excitation of the fluorophore resulting in the generation of carbon dioxide and a second mole of phenol. This is in competition with non-light-producing reactions. The quantitative assessment of the importance of these competing processes has not yet been achieved. However, a determination of the *overall* efficiency of the reaction provides an approximate value for the competition. For the reaction of TCPO–hydrogen peroxide in which 9,10-diphenylanthracene (DPA) is the fluorophore, the overall efficiency is $10^{-4}$ Einstein mol$^{-1}$ of oxalate ($\phi_{CL} = 10^{-4}$). The overall efficiency is the product of the efficiencies for fluorescence of DPA, for chemical production of X (Scheme 3) and for the chemical to electronic energy transfer, i.e.

$$\Phi_{CL} = \phi_F \cdot \phi_X \cdot \phi_{ET}. \quad (8)$$

A partial analysis is possible. Since DPA fluorescence efficiency is known to be quantitative, the $10^4$ loss in efficiency must arise from either the chemistry to produce X or the electronic excitation (CIEEL mechanism) or both. Thus, any improvement in the efficiency of the peroxyoxalate reaction must originate in these two proceses.

One parameter which was considered important was the temperature dependence. However, as shown in Fig. 14, only a modest dependence is noted in the region between 5–50°C. Analyses of these data reveal interesting activation parameters for the reaction. Figure 15 shows that the enthalpy of the rise rate is a modest 2.36 kcal mol$^{-1}$, whereas the

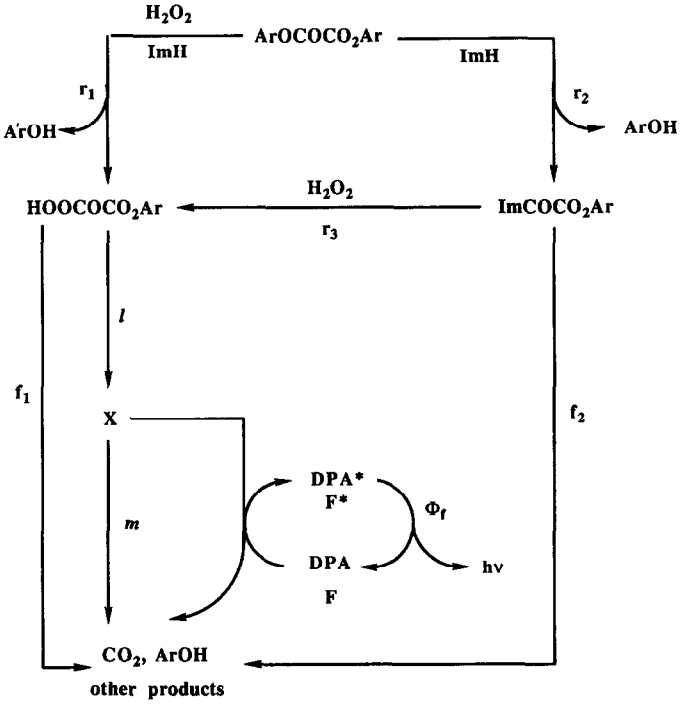


**Scheme 3**
The peroxyoxalate chemiluminescence mechanism. ImH = imidazole, DPA [9, 10] = diphenylanthracene, Ar = 2,4,6-trichlorophenyl and $r_1$, $r_2$, $r_3$, $f_1$, $f$, $l$, $q$ and $m$ are rate constants for the steps indicated.

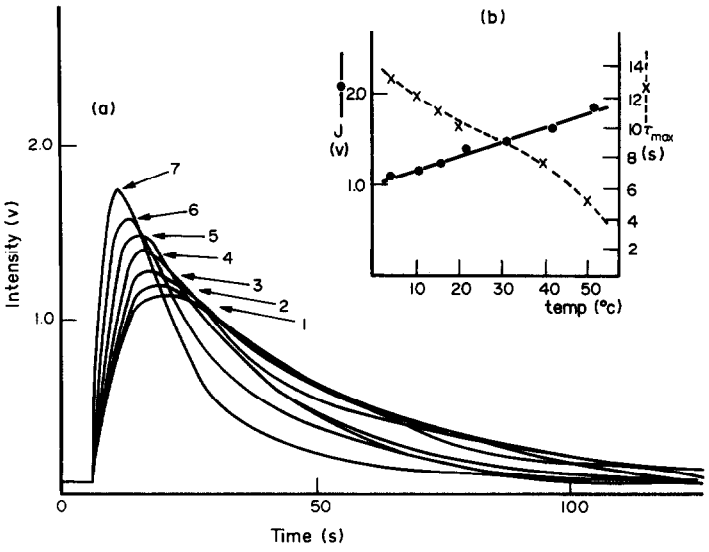


**Figure 14**
(a) Temperature dependence on the time–intensity profile (see ref. 28). Temperatures for the TCPO–hydrogen peroxide reaction were (1) 5, (2) 10, (3) 15, (4) 20, (5) 30, (6) 40, (7) 50°C. Inset (b): The effect of temperature on $J$ and $\tau_{max}$.

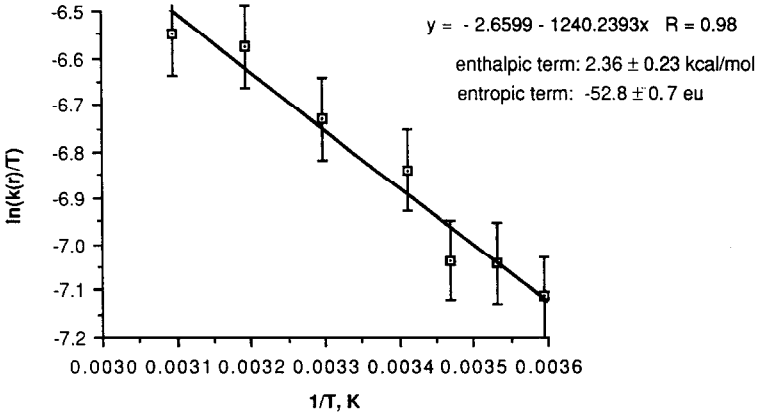


**Figure 15**
Arrhenius plot for the rise rate constant.

entropic contribution is sizeable, $\Delta S^{\neq} = -52.8$ eu. Likewise, the temperature dependence of the fall rate gave values of $\Delta H^{\neq} = 4.50$ kcal mol$^{-1}$ and $\Delta S^{\neq} = -49.6$ eu. These values are suggestive of a rate-limiting electron transfer process for the reaction, in accord with a CIEEL process.

These studies have provided mechanistic insight into the nature of the reaction, but structural details on the intermediate or intermediates were not forthcoming from this work and spectroscopic methods were developed for tracking the intermediate. Here, the availability of the fluoro derivatives, especially the 2,6-difluorophenyl oxalate, provided an opportunity to probe the reaction by more sensitive $^{19}$F NMR techniques. Figure 16 gives the profile of the $^{19}$F NMR spectra as a function of time [28]. Using synthetically derived standards, each $^{19}$F absorption except the weak absorption at −127.7 ppm (B) could be assigned. The major absorptions were the oxalate ester (A), the hydrolysed half-ester (C) and the 2,6-difluorophenol (D).

The absorption at −127.7 ppm was further characterized by its response to added fluorophores and electron donors. As shown in Fig. 17, with addition of dansyl phenylalanine (DNS-phe), a typical substrate for the chemiluminescence-activated process [1], the peak

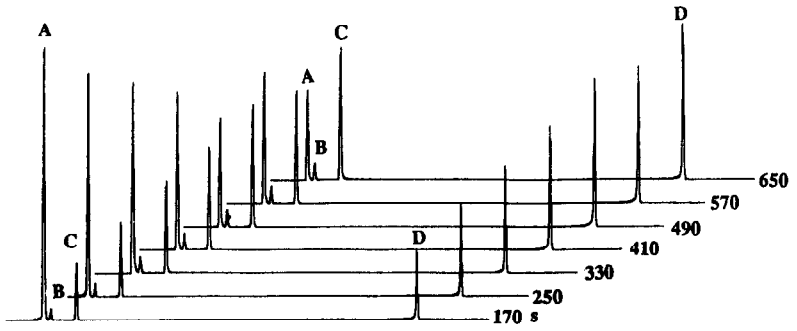


**Figure 16**
$^{19}F$ resonances of DFPO (A), intermediate (B), half ester (C) and DFP (D) monitored for reaction of [DFPO] = 51 mM and $[H_2O_2]$ = 240 mM in 75% aqueous $CD_3CN$. (Reprinted from ref. 28 with permission of *Biomedical Chromatography*.)

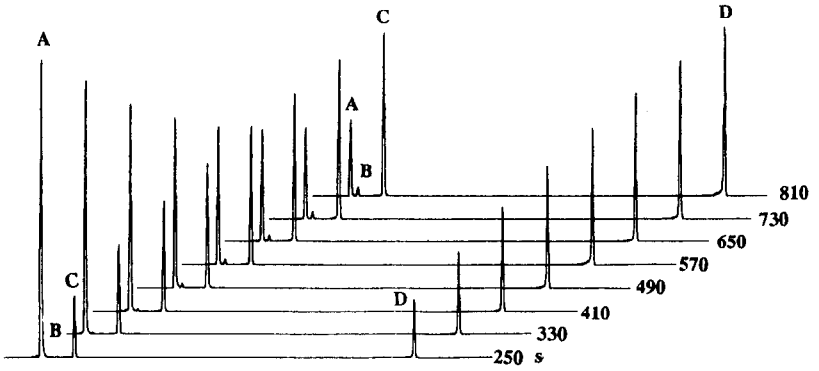


**Figure 17**
$^{19}F$ resonances of DFPO (A), intermediate (B), half ester (C) and DFP (D) monitored for reaction of [DFPO] = 51 mM and $[H_2O_2]$ = 240 mM and [DNS-Phe] = 8 mM in 75% aqueous $CD_3CN$. (Reprinted from ref. 28 with permission of *Biomedical Chromatography*.)

intensity of B decreased inversely as the concentration of DNS-phe increased. The rise and fall of the $^{19}F$ NMR absorption followed an intensity–time profile very similar to that observed for chemiluminescence (Fig. 18). In fact, an overlay of the two time–intensity profiles (NMR and CL) showed identical maxima. The unequal decay profiles probably arise from competing degradation of the dansyl group under the higher concentrations of hydrogen peroxide (240 nM) used in the experiments (Fig. 19).

This evidence suggests that the absorption assigned as B is likely the reactive intermediate X in our earlier mechanistic scheme (Scheme 3). Based on the chemical shift of the absorption relative to those of the partial hydrolysis product and the starting oxalate, it is reasonable to conclude that the reactive intermediate is indeed the peroxyoxalate ester itself and not one of the more exotic structures such as the

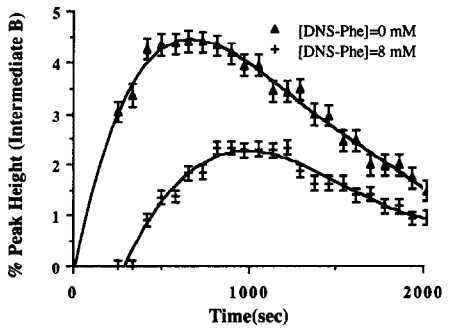


**Figure 18**
Time–intensity plot for the $^{19}F$ NMR signal assigned to intermediate (B).

dioxetanedione or the dioxetane hemiphenolate.

Another useful result of the $^{19}F$ NMR study is the quantitative evaluation of the hydrolytic versus the productive chemiluminescence pathway (Fig. 20). Clearly, hydrolysis to the

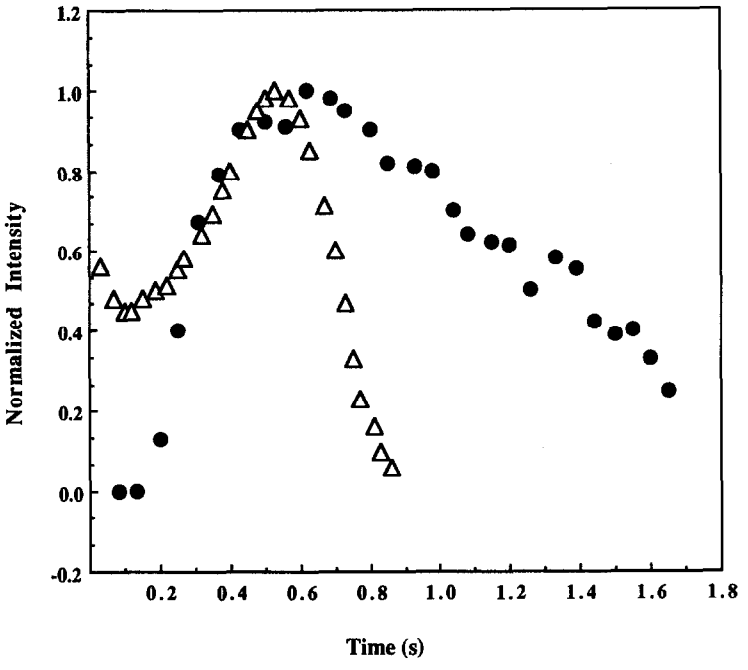


**Figure 19**
Overlay of time–intensity plots for the $^{19}F$ NMR signal for B and the chemiluminescence reaction of 2,6-DFPO–hydrogen peroxide. (The circles represent peroxyoxalate concentration, and the triangles represent chemiluminescence intensity.)

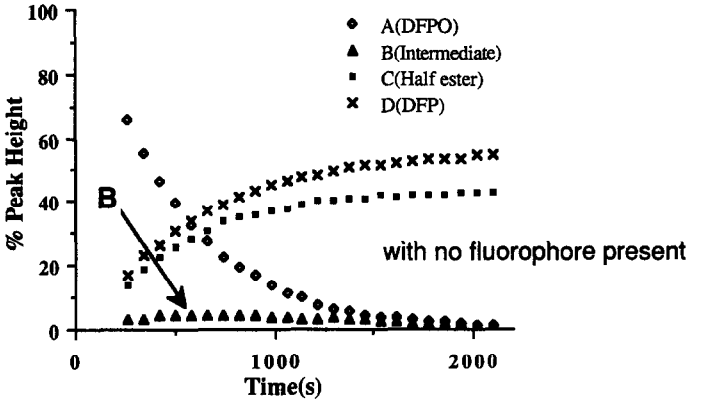


**Figure 20**
Time dependence of the $^{19}F$ NMR absorptions for the DFPO–hydrogen peroxide reaction. DFPO = bis-2,6-difluorophenyloxalate; C = 2,6-difluorophenyl oxalic acid; DF = 2,6-difluorophenol.

half-ester is the major reaction pathway. In fact, it consumes 90% of the oxalate ester. Thus, hydrolysis accounts for approximately a factor of 10 loss in the chemiluminescence efficiency.

Finally, a recent report by Zech and Wong [11] on the determination of phenylalanyl-neurotensin (a 13-amino acid peptide) in human blood plasma is illustrative of the potential of chemiluminescence detection coupled with the NDA/CN derivatization processes. The neurotensins have one lysine residue containing a primary-amino group which rapidly reacts with NDA/CN to form a highly fluorescent CBI derivative. The complex plasma mixture was resolved by a cyanopropyl and $C_{18}$ column-switching arrangement. The eluent was monitored sequentially by fluorescence and chemiluminescence detectors for direct comparison of sensitivity. The results

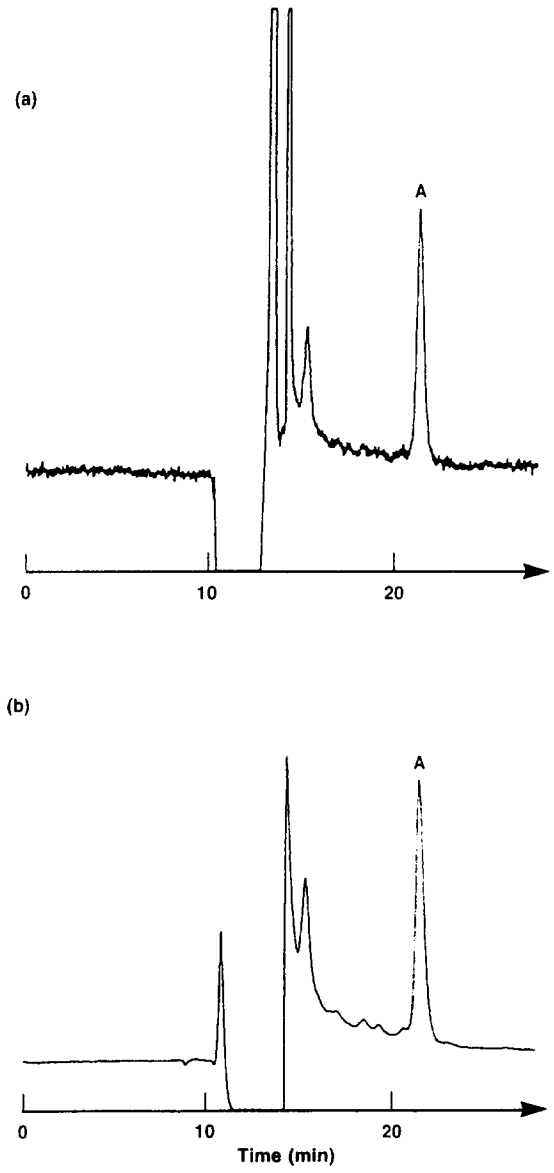


**Figure 21**
Detection of phenylalanyl-NTS (A) in human blood plasma on a 10 cm × 4.6 mm, 5 μm CN (ES Industries) [mobile phase: MeOH–50 mM sodium acetate, pH 4.0 (1:1, v/v)] and 15 cm × 4.6 mm 5 μm TSK-ODS $C_{18}$ [mobile phase: acetonitrile–10 mM imidazole, pH 7.0 (38:62, v/v)] columns in tandem. (a) Fluorescence detector: Shimadzu RF-530; $\lambda_{ex}$ = 420 nm; $\lambda_{em}$ = 490 nm. (b) Chemiluminescence detector: Atto Biometer AC-2220. CL reagents (conc.): TCPO (0.5 M); $H_2O_2$ (0.05 M). (Reprinted with permission of LC–GC, ref. 29.)

(Fig. 21) show that an order of magnitude improvement in signal-to-noise is possible when CL detection is employed.

The neurotensin and enkephalin examples illustrate the current level of signal-to-noise enhancement that can be expected for chemiluminescence. The potential for improvement is very great, however, when one realizes that the chemiluminescence yield from the oxalate–hydrogen peroxide reaction is no better than 0.1%. Improvement and modification of the CL reaction are being actively pursued at the Center.

*Acknowledgements* — The work reported here was supported in part by the Kansas Technology Enterprise Corporation, The Center for Bioanalytical Research, Oread Laboratories and the National Institute on Drug Abuse (DA04740). Contributions from Drs O. Wong, S. Lunte, M. Orlovic and S. Crowley are gratefully acknowledged.

## References

[1] S. Kobayashi and K. Imai, *Anal. Chem.* **52**, 424–427 (1980).
[2] G. Mellbin, *J. Liq. Chromatogr.* **6**, 1603–1616 (1983).
[3] K.W. Sigvardson and J.W. Birks, *Anal. Chem.* **55**, 432–435 (1983).
[4] G.J. De Jong, N. Lammers, F.J. Spruit, U.A.Th. Brinkman and R.W. Frei, *Chromatographia* **18**, 129–133 (1984).
[5] T. Koziol, M.L. Grayeski and R. Weinberger, *J. Chromatogr.* **317**, 355–366 (1984).
[6] P. de Montigny, J.F. Stobaugh, R.S. Givens, R.G. Carlson, K. Srinivasachar, L.A. Sternson and T. Higuchi, *Anal. Chem.* **59**, 1096–1101 (1987).
[7] R.G. Carlson, K. Srinivasachar, R.S. Givens and B.K. Matuszewski, *J. Org. Chem.* **51**, 3978–3983 (1986).
[8] B.K. Matuszewski, R.S. Givens, K. Srinivasachar, R.G. Carlson and T. Higuchi, *Anal. Chem.* **59**, 1102–1105 (1987).
[9] M.C. Roach and M.D. Harmony, *Anal. Chem.* **59**, 411–415 (1987).
[10] T. Kawasaki, T. Higuchi, K. Imai and O.S. Wong, *Anal. Biochem.* **180**, 279 (1989).
[11] L. Zech and O.S. Wong, *Pharm. Res.* **5**, S-15, Abstr. No. 327 (1988).
[12] J.F. Stobaugh and S.C. Crowley, *Pharm. Res.* **5**, S-15, Abstr. No. 342 (1988).
[13] R.S. Givens, R.L. Schowen, J. Stobaugh, T. Kuwana, F. Alvarez, N. Parekh, B. Matuszewski, T. Kawasaki, O. Wong, M. Orlovic, H. Chokshi and K. Nakashima, ACS Symposium Series No. 383, (M.C. Goldberg, Ed.). American Chemical Society, Washington, DC (1989).
[14] M. Roth, *Anal. Chem.* **43**, 880–882 (1971).
[15] S.S. Simons Jr and D.F. Johnson, *J. Am. Chem. Soc.* **98**, 7098–7099 (1976).
[16] S.S. Simons Jr and D.F. Johnson, *J. Chem. Soc., Chem. Commun.* 374–375 (1977).
[17] J.F. Stobaugh, P. de Montigny, S.C. Crowley and A. Thakur, *Pharmaceut. Res.* **5**, S-15, Abstr. No. 341 (1988).
[18] M. Mifune, D.K. Krehbeil, J.F. Stobaugh and C.M. Riley, *J. Chromatogr.* **496**, 55–70 (1989).
[19] M.M. Rauhut, L.J. Bollyky, B.G. Roberts, M. Loy, R.H. Whitman, A.V. Iannotta, A.M. Semsel and R.A. Clarke, *J. Am. Chem. Soc.* **89**, 6515–6522 (1967).
[20] F. McCapra, K. Perring, R.J. Hard and R.A. Hann, *Tetrahedron Lett.* 5087–5091 (1981).
[21] R.S. Givens and R.L. Schowen, in *Chemiluminescence and Photochemical Reaction Detection in*

*Chromatography* (J.W. Birks, Ed.), Chap. 5, pp. 125–148. VCH, New York (1989).
[22] G.B. Schuster and S.P. Schmidt, *Adv. Phys. Org. Chem.* **18**, 187–238 (1982).
[23] M. Orlovic, R.L. Schowen, R.S. Givens, F. Alvarez, B. Matuszewski and N. Parekh, *J. Org. Chem.* **54**, 3606–3610 (1989).
[24] C.L.R. Catherall, T.F. Palmer and R.B. Cundall, *J. Chem. Soc. Faraday Trans. II* **80**, 823–836, 837–849 (1984).
[25] F.J. Alvarez, N.J. Parekh, B. Matuszewski, R.S. Givens, T. Higuchi and R.L. Schowen, *J. Am. Chem. Soc.* **108**, 6435–6437 (1986).
[26] B. Matuszewski, R.S. Givens, R.G. Carlson, T. Kawasaki and O.S. Wong, U.S. Patent 4,758,520; Ser. No. 837,671, 6-19-1988.
[27] N. Hanaoka, R.S. Givens, R.L. Schowen and T. Kuwana, *Anal. Chem.* **60**, 2193–2197 (1989).
[28] H.P. Chokshi, M. Barbush, R.G. Carlson, R.S. Givens, T. Kuwana and R.L. Schowen, *Biomed. Chromatogr.* (1990). In press.
[29] S.M. Lunte and O.S. Wong, *LC–GC* **7**, 908–913 (1989).

[*Received for publication 11 July 1990*]